Next-to-leading order QCD predictions for W+1 jet and W+2 jet production with at least one b jet at the 7 TeV LHC

J. M. Campbell, F. Caola, F. Febres Cordero, L. Reina, and D. Wackeroth

Phys. Rev. D **86**, 034021 — Published 24 August 2012

DOI: 10.1103/PhysRevD.86.034021

FERMILAB-PUB-11-325-T
NSF-KITP-11-134

NLO QCD predictions for $W + 1$ jet and $W + 2$ jet production with at least one b jet at the 7 TeV LHC

J. M. Campbell,[1] **F. Caola**,[1,2,3] **F. Febres Cordero**,[4] **L. Reina**,[5,7] and **D. Wackeroth**[6,7]

[1]Theoretical Physics Department, Fermi National Accelerator Laboratory
P. O. Box 500, Batavia, IL 60510

[2]Dipartimento di Fisica, Università di Milano and INFN, Sezione di Milano,
Via Celoria 16, I-20133 Milano, Italy

[3] Department of Physics and Astronomy, Johns Hopkins University, Baltimore, MD
21218-2686

[4]Departamento de Fisica, Universidad Simon Bolivar
Caracas 1080A, Venezuela

[5]Physics Department, Florida State University, Tallahassee, FL
32306-4350

[6]Department of Physics, SUNY at Buffalo, Buffalo, NY
14260-1500

[7]KITP, University of California Santa Barbara, CA 93106-4030, USA

Abstract

We provide predictions for the production of a W boson in association with up to two jets including at least one b-jet at next-to-leading order (NLO) in QCD at the CERN Large Hadron Collider with 7 TeV center-of-mass energy. Both exclusive and inclusive event cross section and b-jet cross sections are presented. The calculation is performed consistently in the five-flavor-number scheme where both $q\bar{q}'$ and bq $(q \neq b)$ initiated parton level processes are included at NLO QCD. We study the residual theoretical uncertainties of the NLO predictions due to the renormalization and factorization scale dependence, to the uncertainty from the parton distribution functions, and to the values of α_s and the bottom-quark mass.

1 Introduction

The study of W-boson production in association with one and two b jets at both the Fermilab Tevatron collider ($p\bar{p}$) and the CERN Large Hadron Collider (LHC, pp) has many interesting experimental and theoretical facets. On the experimental side, these processes are backgrounds to WH production with the Higgs boson decaying to b quarks, to single-top and top-pair production, and to many new physics searches. On the theoretical side, these processes offer an interesting testing ground for calculational techniques involving heavy quarks with a non-negligible initial-state parton density. Predictions for W-boson production in association with b quarks are available at higher order in QCD using various calculational techniques (four-flavor [1, 2, 3, 4] and five-flavor number schemes [5]) and approximations (massless [1, 5] and massive b quarks [2, 3, 4]). Recently, NLO fixed-order calculations of the $q\bar{q}' \to Wb\bar{b}$ parton-level process with massive b quarks have been interfaced with parton-shower Monte Carlo programs within the POWHEG [6] and MC@NLO [4] frameworks.

In this context, the predictions for $W+1$ jet and $W+2$ jet production with at least one b jet include processes where b quarks can have low transverse momentum so that finite b-quark mass effects become important. Assuming only massless quarks and gluons in the initial state (i.e. working in a four-flavor-number scheme), this signature can only originate from the diagram in Fig. 1(a), i.e. from $q\bar{q}' \to Wb\bar{b}$, and its higher-order corrections. The calculation of NLO QCD corrections to $q\bar{q}' \to Wb\bar{b}$ of Fig. 1(a) with massive b quarks has been provided in [2, 3, 4], and made available in MCFM [7]. It exhibits interesting theoretical features. In particular, large logarithms of the form $\alpha_s \log(m_b/\mu)$ (where μ is a scale of the order of the maximum b-quark transverse momentum) originate from the splitting of a gluon into two almost collinear bottom quarks. This happens for the first time in the parton-level process $qg \to Wb(\bar{b})q'$ (where $(\bar{b})$ denotes an untagged low p_T $\bar{b}$ quark) depicted in Fig. 2. This process arises as part of the NLO QCD corrections to $q\bar{q}' \to Wb\bar{b}$, but it is intrinsically a tree-level process. As such it exhibits a large renormalization (μ_R) and factorization (μ_F) scale dependence and, because it is enhanced by large logarithms of the form $\alpha_s \log(m_b/\mu)$, it potentially introduces a large systematic uncertainty in the calculation, that could be tamed only by a complete next-to-next-to-leading (NNLO) calculation of $q\bar{q}' \to Wb\bar{b}$. A clever way to reduce this problem is to introduce a b-quark parton distribution function (PDF) [9, 10], defined purely perturbatively as originating from gluon splitting. In this way, the scale evolution of the b-quark PDF resums the large logarithms originating at each order and provides a more stable, although approximate solution. In this approach, the LO process is considered to be $bq \to Wbq'$, as shown in Fig. 1(b), where the b-quark PDF is generated perturbatively from the gluon PDF and the Altarelli-Parisi splitting function for $g \to b\bar{b}$ splitting, and the $\bar{b}$ is assumed to have too low a p_T to be observable. This results in exactly the process shown in Fig. 2 with a low-p_T b quark. In this approach, the b quark is treated as massless in the hard scattering process $qb \to Wbq'$, the so-called (simplified) ACOT scheme [9, 10], and its mass only appears as a collinear regulator in the initial $g \to b\bar{b}$ splitting function. The resulting logarithms $\alpha_s \ln(m_b/\mu_F)$ are resummed via DGLAP evolution of the b-quark PDF. The NLO QCD calculation of $qb \to Wbq'$ has been performed in Ref. [5] and made available in MCFM [7]. In fact, as explained in [8], the two tree level processes, $q\bar{q}' \to Wb\bar{b}$ and $qb \to Wbq'$ and their $O(\alpha_s)$ corrections can be combined, as long as sufficient care is taken to subtract logarithmic terms that would otherwise be double counted.

In this paper we will combine NLO QCD calculations of $q\bar{q}' \to Wb\bar{b}$ and $qb \to Wbq'$ parton level processes including b-quark mass effects to provide precise predictions for $W+1$ jet and $W+2$ jet production with at least one b jet at the 7 TeV LHC. The choice of the experimental signature, jet algorithm, and kinematic cuts has been made according to ATLAS specifications [11]. We will closely follow Ref. [8] where a consistent combination of these two NLO calculations has been performed for the first time to provide predictions for the production of a W boson and one b-jet. It is interesting to note that the calculation of Ref [8] has been compared with a measurement of the b-jet cross section of W-boson production in association with one and two b jets by the CDF collaboration at the Tevatron [14]. This comparison found a discrepancy of about two standard deviations [12, 13].

After a brief presentation of the theoretical framework in Section 2, we will discuss NLO QCD predictions and their residual uncertainties for the 7 TeV LHC in Section 3 and present our conclusions in Section 4.

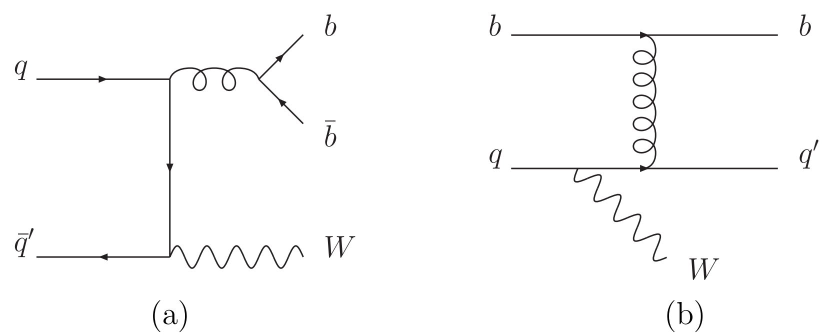

Figure 1: Leading-order parton-level processes for the production of a W boson and one or two jets with at least one b jet.

2 Theoretical Framework

The predictions presented in this paper are based on the combination of NLO QCD calculations of the $q\bar{q}' \to Wb\bar{b}$ [2, 3, 7] and $bq \to Wbq'$ [5] parton-level processes, as presented in Ref. [8] and implemented in MCFM [7] (where the leptonic W decay is included), and we refer to [8] for more details.

In the NLO QCD calculation of the $q\bar{q}' \to Wb\bar{b}$ process the b quark is considered to be massive, and only light quarks ($q \neq b$) are considered in the initial state, i.e. the so-called four-flavor number scheme (4FNS) is used. In the NLO QCD calculation of the $bq \to Wbq'$ process the b-quark mass is only kept as regulator of the collinear singularity while it is neglected in the hard process so that the hadronic cross section is obtained as follows,

$$\sigma_{bq}^{NLO} = \int dx_1 dx_2 b(x_1, \mu) \left[\sum_q q(x_2, \mu_F) \hat{\sigma}_{bq}^{NLO}(m_b = 0) + g(x_2, \mu_F) \hat{\sigma}_{bg}^{LO}(m_b = 0) \right] \quad . \tag{1}$$

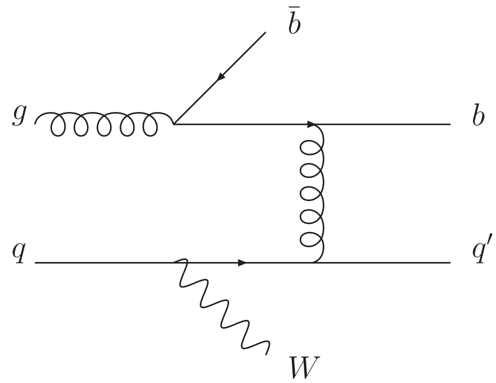

Figure 2: A parton-level process contributing to Wbj production that appears at NLO in the calculation of $\mathcal{O}(\alpha_s)$ corrections to $q\bar{q}' \to Wb\bar{b}$. This process is also equivalent to the LO b-quark initiated process of Fig. 1(b), with the b quark originating from collinear $g \to b\bar{b}$ splitting. The consistent treatment of this process in the combination of the two NLO calculations is described in Section 2.

An approximate solution of the DGLAP evolution equation for the b-quark PDF $b(x, \mu_F)$ with initial condition $b(x, \mu_F) = 0$ at $\mu_F = m_b$ exhibits the collinear logarithm at leading order in α_s as follows [9, 10],

$$\tilde{b}(x, \mu_F) = \frac{\alpha_s(\mu_R)}{\pi} \log\left(\frac{\mu_F}{m_b}\right) \int_x^1 \frac{dz}{z} P_{qg}(z) g\left(\frac{x}{z}, \mu_F\right) \quad . \tag{2}$$

When combining the NLO calculation of $bq \to Wbq'$ with the NLO calculation of $q\bar{q}' \to Wb\bar{b}$ this part of the b-quark PDF has to be subtracted in order to avoid double counting of the process of Fig. 2 which is already included in the 4FNS NLO QCD calculation. The full five-flavor number scheme (5FNS) result at NLO QCD, including an all order resummation of collinear initial-state logarithms via DGLAP evolution, is then obtained schematically as follows,

$$\begin{aligned} \sigma^{NLO}_{\text{5FNS}} &= \sigma^{NLO}_{4FNS}(m_b \neq 0) + \sigma^{NLO}_{bq} \\ &- \sum_q \int dx_1 dx_2 \tilde{b}(x_1, \mu_F) q(x_2, \mu_F) \hat{\sigma}^{LO}_{bq}(m_b = 0) \quad . \end{aligned} \tag{3}$$

Note that the NLO computations of the $q\bar{q}' \to Wb\bar{b}$ and $bq \to Wbq'$ processes in Eq. (3) have been both performed in the $\overline{\text{MS}}$ renormalization scheme. We assume the number of light flavors to be $n_{lf} = 5$ in both the running of $\alpha_s(\mu_R)$ and in the determination of the one-loop gluon self energy, Σ_{gg}, i.e. we only decouple the top quark from the running of α_s in the modified $\overline{\text{MS}}$ scheme. This choice is motivated by the fact that we usually choose renormalization scales μ_R considerably larger than m_b. Alternatively, one can choose to include the b-quark mass in the calculation of Σ_{gg} (as done in the implementation of $q\bar{q}' \to Wb\bar{b}$ in POWHEG [6]) and/or also decouple the b quark ($n_{lf} = 4$). The different treatments generally result in differences of about a few per cent in the cross sections presented in Section 3.

We now present the sub-processes relevant for our analysis. In detail, σ_{4FNS}^{NLO} and σ_{bq}^{NLO} in this paper include the following parton level processes:

$$\sigma_{4FNS}^{NLO} \quad \begin{array}{l} q\bar{q}' \to Wb\bar{b} \text{ at tree level [Fig. 1(a)] and one loop } (m_b \neq 0) \\ q\bar{q}' \to Wb\bar{b}g \text{ at tree level } (m_b \neq 0) \\ gq \to Wb\bar{b}q' \text{ at tree level (Fig. 2), } (m_b \neq 0) \end{array}$$

$$\sigma_{bq}^{NLO} \quad \begin{array}{l} bq \to Wbq' \text{ at tree level [Fig. 1(b)] and one loop } (m_b = 0) \\ bq \to Wbq'g \text{ at tree level } (m_b = 0) \\ bg \to Wbq'\bar{q} \text{ at tree level } (m_b = 0) \end{array}$$

We present results for $\sigma_{\rm 5FNS}^{NLO}$ and σ_{4FNS}^{NLO} separately in Tables 2-3 for the signatures described in the following section. We leave a full discussion of these results until Section 3, but here simply note that the scale dependence of the difference $\sigma_{\rm 5FNS}^{NLO} - \sigma_{4FNS}^{NLO}$ clearly shows the impact of the initial-state collinear logarithms. The difference is negligible for scales of the order of the b-quark mass but can amount to about 40% of $\sigma_{\rm 5FNS}^{NLO}$ for $\mu \approx 360$ GeV.

Note that we do not include contributions to Wbj production which arise from $c \to Wb$ transitions (we assume $V_{cb} = 0$), since these contributions are suppressed by the smallness of V_{cb} and the charm-quark PDF. For instance, the dominant contribution to Wbj production at the LHC when considering $|V_{cb}| = 0.04$ is expected to be $cg \to Wbg$. Using the setup of Table 1 we found for the inclusive W^+b event cross section at LO QCD with $\mu = \mu_0$: $290 \times |V_{cb}|^2 = 0.5$ pb, which is about 1% of the result presented in Table 2.

3 Results

Predictions are provided for $W + 1$ jet and $W + 2$ jet production where at least one jet is a $b-$jet as has been measured by ATLAS at the 7 TeV LHC [11]. Jets are clusters of partons built using the anti-k_T algorithm which passed the kinematic cuts specified in Table 1. In the following, b denotes a jet containing one b quark or one $\bar{b}$ antiquark, while (bb) denotes a jet containing a b and $\bar{b}$ quark. b and (bb) jets may also contain a light parton. j labels a jet without b quarks. We will provide predictions for event and b-jet cross sections for the following signatures:

- Wb inclusive: one and two-jet events with b jets containing a single b, i.e. $Wb+Wbj+Wb\bar{b}$.
- $W(bb)$ inclusive: one and two-jet events with one (bb) jet, i.e. $W(bb) + W(bb)j$. This signature can only result from processes contributing to σ_{4FNS}^{NLO} listed in Section 2.
- Wb exclusive: one-jet events with one b jet containing a single b, i.e. Wb.
- $W(bb)$ exclusive: one-jet events with one (bb) jet, i.e. $W(bb)$. This signature can only result from the processes contributing to σ_{4FNS}^{NLO} listed in Section 2.

The event and b-jet cross sections have been obtained consistently at NLO in the 5FNS following Ref. [8] and as briefly described in Section 2.

Table 1: Kinematic cuts, jet finding algorithm, PDF sets and input parameters used in this study, if not stated otherwise. The kinematic cuts used to simulate the acceptance and resolution of the detectors are chosen according to ATLAS specifications [11].

7 TeV LHC:	$p_{Tj} > 25$ GeV	$\|y_j\| < 2.1$
anti$-k_T$ jet algorithm		$p = -1, R = 0.4$
$M_W = 80.41$ GeV		$m_b = 4.7$ GeV
LO: CTEQ6L1		NLO: CTEQ6.6 [15]
$\alpha_S^{LO}(M_Z) = 0.130$		$\alpha_S^{NLO}(M_Z) = 0.118$
$g_w^2 = 8M_W^2 G_F/\sqrt{2} = 0.4266177$		$G_F = 1.16639 \times 10^{-5}$ GeV^{-2}
$V_{ud} = V_{cs} = 0.974$		$V_{us} = V_{cd} = 0.227$ $\quad (V_{ub} = V_{cb} = 0)$

If not stated otherwise, all results are obtained assuming $\mu_R = \mu_F = \mu$, where μ_R and μ_F denote the renormalization and factorization scales respectively. We vary μ between $\mu_0/4$ and $4\mu_0$ with $\mu_0 = M_W + 2m_b$. Results for the event cross sections corresponding to the four signatures described above are given in Tables 2-3, where we consider non-decaying W bosons. The theoretical uncertainty due to the scale dependence can be estimated using these results. Inclusive and exclusive event cross sections for $pp \to W^\pm bX \to e^\pm \nu bX$ assuming $\mu = \mu_0$ are provided in Table 4. The results have been obtained by multiplying the total cross sections of Tables 2-3 with the branching ratio BR($W^\pm \to e^\pm \nu$) = 0.10805 (labeled as "no cuts") [1] and by requiring ATLAS inspired lepton cuts, $p_T^e > 20$ GeV, $|\eta^e| < 2.5$, $p_T^\nu > 25$ GeV, $m_T^W > 40$ GeV, $R(l,j) > 0.5$ (labeled as "ATLAS cuts"). All these cuts are implemented in the full NLO computation including W decay of MCFM [7].

The combined PDF and α_s uncertainties (at 68% C.L.) are estimated using the NNPDF2.1 [17], CTEQ6.6 [15, 16], and MSTW08 [18] sets of PDFs as presented in Tables 5-6. The combination of the PDF and α_s errors is done according to the PDF4LHC NLO prescription [19]. The dependence of our predictions on the value of the b-quark mass is at the level of a few percent, as can be seen from Tables 7-8.

The predictions for the event cross sections for $W+1$ jet and $W+2$ jets with at least one b (or (bb)) jet, denoted as σ_{1j+2j}, $W+1b$ jet (or (bb) jet), denoted as σ_{1j}, and $W+2$ jets with at least one b (or (bb)) jet, denoted as σ_{2j}, are provided separately in Table 9. They are obtained from the results of Tables 2-3 as follows:

$$\begin{aligned}
\sigma_{1j+2j} &= [\sigma_{\text{event}}(Wb\,\text{incl.}) + \sigma_{\text{event}}(W(bb)\,\text{incl.})] \\
\sigma_{1j} &= [\sigma_{\text{event}}(Wb\,\text{excl.}) + \sigma_{\text{event}}(W(bb)\,\text{excl.})] \\
\sigma_{2j} &= \sigma_{1j+2j} - \sigma_{1j}
\end{aligned}$$

The b-jet cross sections for $W+1$ jet and $W+2$ jets with at least one b jet are provided separately in Table 10. They can be obtained from the Wb and $W(bb)$ inclusive event cross sections of Table 2 when the $Wb\bar{b}$ contribution (normally included in the Wb inclusive

[1] Note that the difference between this approximation and the full calculation of the $pp \to e^\pm \nu bX$ cross section is of the order of $\Gamma_W/M_W \approx 2.5\%$.

Table 2: Inclusive event cross sections (in pb), LHC ($\sqrt{s} = 7$ TeV). No branching ratios or tagging efficiencies are included. The Monte Carlo integration error is 0.5%.

	W^+b incl.		$W^+(bb)$ incl.	W^-b incl.		$W^-(bb)$ incl.
	5FNS	4FNS	4FNS	5FNS	4FNS	4FNS
$\mu = \mu_0/4$	66.3	67.3	18.6	40.8	41.2	11.4
$\mu = \mu_0/2$	60.4	52.5	13.8	37.2	32.2	8.6
$\mu = \mu_0$	56.7	42.6	10.9	34.8	26.3	6.8
$\mu = 2\mu_0$	53.2	35.5	8.8	32.7	21.9	5.4
$\mu = 4\mu_0$	50.0	30.1	7.4	30.7	18.7	4.5

Table 3: Exclusive event cross sections (in pb), LHC ($\sqrt{s} = 7$ TeV). No branching ratios or tagging efficiencies are included. The Monte Carlo integration error is within 0.5%.

	W^+b excl.		$W^+(bb)$ excl.	W^-b excl.		$W^-(bb)$ excl.
	5FNS	4FNS	4FNS	5FNS	4FNS	4FNS
$\mu = \mu_0/4$	36.7	36.9	9.4	22.8	22.3	5.7
$\mu = \mu_0/2$	35.3	35.2	7.8	21.8	21.5	4.9
$\mu = \mu_0$	33.9	26.2	6.7	20.7	16.2	4.3
$\mu = 2\mu_0$	32.2	22.8	5.9	19.8	14.2	3.7
$\mu = 4\mu_0$	30.3	19.9	5.2	18.8	12.5	3.3

signatures) is counted twice (since it contains two b jets). More explicitly, using the $Wb\bar{b}$ cross section separately provided in Table 9 in parentheses, the b-jet cross section can be obtained from the event cross sections in Table 2 as follows

$$\begin{aligned}
\sigma_{b-\text{jet}} &= \left[\sigma_{\text{event}}(Wb\,\text{incl.}) - \sigma_{\text{event}}(Wb\bar{b})\right] + 2\,\sigma_{\text{event}}(Wb\bar{b}) + \sigma_{\text{event}}(W(bb)\,\text{incl.}) \\
&= \sigma_{\text{event}}(Wb\,\text{incl.}) + \sigma_{\text{event}}(Wb\bar{b}) + \sigma_{\text{event}}(W(bb)\,\text{incl.}) \\
&= \sigma_{1j+2j} + \sigma_{\text{event}}(Wb\bar{b})
\end{aligned}$$

4 Conclusions

In this paper we have computed the cross section for the production of a W boson in association with up to two jets, including at least one b-jet, at the 7 TeV LHC. The calculation consistently combines next-to-leading order corrections to the parton level processes $q\bar{q}' \to Wb\bar{b}$ [2, 3, 7] and $bq \to Wbq'$ [5] according to the procedure presented in Ref. [8]. We have particularly focused on performing a systematic study of our prediction, considering a number of sources of theoretical uncertainty, under a set of cuts that have been used by the ATLAS collaboration [11].

	Wb incl.		$W(bb)$ incl.	Wb excl.		$W(bb)$ excl.
	4FNS	5FNS	4FNS	4FNS	5FNS	4FNS
W^+ no cuts	4.6	6.1	1.2	2.8	3.7	0.7
W^+ ATLAS cuts	2.2	2.8	0.5	1.3	1.7	0.3
W^- no cuts	2.8	3.8	0.7	1.8	2.2	0.5
W^- ATLAS cuts	1.3	1.6	0.3	0.8	1.0	0.2

Table 4: Inclusive and exclusive event cross sections (in pb), LHC ($\sqrt{s} = 7$ TeV), for $pp \to W^{\pm}bX \to e^{\pm}\nu bX$ (with $\mu = \mu_0$ and CTEQ6.6 [15]). The "no cuts" result is obtained by multiplying the total cross sections of Table 2 and Table 3, respectively, with the branching ratio BR($W^{\pm} \to e^{\pm}\nu$) = 0.10805. The "ATLAS cuts" result is obtained by requiring $p_T^e >$ 20 GeV, $|\eta^e| < 2.5$, $p_T^{\nu} > 25$ GeV, $m_T^W > 40$ GeV, $R(l,j) > 0.5$. All these cuts are implemented in the full NLO computation including W decay of MCFM [7].

	W^+b incl.		$W^+(bb)$ incl.	W^-b incl.		$W^-(bb)$ incl.
	4FNS	5FNS	4FNS	4FNS	5FNS	4FNS
NNPDF2.1 [17]	44.1	59.2 ± 1.7	11.4 ± 0.3	27.6	36.2 ± 1.0	7.1 ± 0.2
CTEQ6.6 [15, 16]	42.6	56.7 ± 2.1	10.9 ± 0.3	26.3	34.8 ± 1.3	6.8 ± 0.2
MSTW2008 [18]	44.2	59.8 ± 1.7	11.5 ± 0.3	28.6	37.9 ± 1.0	7.4 ± 0.2

Table 5: Inclusive event cross sections (in pb) for different PDF sets including PDF+α_s uncertainties at 68% C.L., determined according to the PDF4LHC NLO prescription [19] (with $\mu_R = \mu_F = \mu_0$).

	W^+b excl.		$W^+(bb)$ excl.	W^-b excl.		$W^-(bb)$ excl.
	4FNS	5FNS	4FNS	4FNS	5FNS	4FNS
NNPDF2.1 [17]	26.5	34.9 ± 1.1	7.0 ± 0.2	16.9	21.6 ± 0.6	4.4 ± 0.1
CTEQ6.6 [15, 16]	26.2	33.9 ± 1.3	6.7 ± 0.2	16.2	20.7 ± 0.9	4.3 ± 0.2
MSTW2008 [18]	27.4	35.6 ± 1.0	7.1 ± 0.2	17.6	22.4 ± 0.7	4.6 ± 0.1

Table 6: Exclusive event cross sections (in pb) for different PDF sets including PDF+α_s uncertainties at 68% C.L., determined according to the PDF4LHC NLO prescription [19] (with $\mu_R = \mu_F = \mu_0$).

	W^+b incl.		$W^+(bb)$ incl.	W^-b incl.		$W^-(bb)$ incl.
	4FNS	5FNS	4FNS	4FNS	5FNS	4FNS
$m_b = 4.2$ GeV	44.8	58.4	12.8	27.7	35.8	7.9
$m_b = 5.0$ GeV	40.8	55.7	10.0	25.2	34.0	6.2

Table 7: Inclusive event cross sections (in pb) for different values of the b quark mass (m_b) obtained with the CTEQ6.6 PDF set [15] and $\mu_R = \mu_F = \mu_0$.

	W^+b excl.		$W^+(bb)$ excl.	W^-b excl.		$W^-(bb)$ excl.
	4FNS	5FNS	4FNS	4FNS	5FNS	4FNS
$m_b = 4.2$ GeV	27.8	35.3	8.0	17.2	21.5	5.0
$m_b = 5.0$ GeV	25.0	33.3	6.1	15.5	20.2	3.8

Table 8: Exclusive event cross sections (in pb) for different values of the b quark mass (m_b) obtained with the CTEQ6.6 PDF set [15] and $\mu_R = \mu_F = \mu_0$.

Table 9: Event cross sections (in pb), LHC ($\sqrt{s} = 7$ TeV) for $W+1$ and $W+2$ jet production with at least one b jet, $W + 1$ b jet, and $W + 2$ jets with at least one b jet (where here b jet denotes a jet with a single b or (bb) pair). The event cross sections for $Wb\bar{b}$ are provided separately in parentheses. No branching ratios or tagging efficiencies are included. The Monte Carlo integration error is within 0.5%.

	W^+_{1j+2j}	W^+_{1j}	W^+_{2j}	W^-_{1j+2j}	W^-_{1j}	W^-_{2j}
$\mu = \mu_0/4$	84.9 [5.6]	46.1	38.8	52.2 [3.2]	28.5	23.7
$\mu = \mu_0/2$	74.2 [5.3]	43.1	31.1	45.8 [3.1]	26.7	19.1
$\mu = \mu_0$	67.6 [5.0]	40.6	27.0	41.6 [2.9]	25.0	16.6
$\mu = 2\mu_0$	62.0 [4.6]	38.1	23.9	38.1 [2.7]	23.5	14.6
$\mu = 4\mu_0$	57.4 [4.2]	35.5	21.9	35.2 [2.5]	22.1	13.1

Our results can be summarized as follows, where we have put together all sources of uncertainty considered in this paper. The event cross sections for W-boson production with one or two jets with at least one b jet at NLO QCD at the LHC (7 TeV) as has been measured by ATLAS [11] (unfolded) is,

$$\sigma_{1j}(W^+ + W^-) = 65.6\ ^{+9.0}_{-8.0}\,(\text{scale})\ ^{+5.3}_{-1.6}\,(\text{PDF} + \alpha_s)\ ^{+4.2}_{-2.2}\,(m_b)\ \text{pb}$$

$$\sigma_{2j}(W^+ + W^-) = 43.6\ ^{+18.9}_{-8.6}\,(\text{scale})\ ^{+5.6}_{-3.0}\,(\text{PDF} + \alpha_s)\ ^{+1.5}_{-1.1}\,(m_b)\ \text{pb}$$

$$\sigma_{1j+2j}(W^+ + W^-) = 109.2\ ^{+27.9}_{-16.6}\,(\text{scale})\ ^{+9.4}_{-2.5}\,(\text{PDF} + \alpha_s)\ ^{+5.7}_{-3.3}\,(m_b)\ \text{pb}$$

The central value corresponds to the CTEQ6.6 PDF set, with $\alpha_s(M_Z) = 0.118$, $\mu = \mu_0 = M_W + 2m_b$ and $m_b = 4.7$ GeV. In the assessment of the theoretical uncertainty we have considered a very conservative scale variation from $\mu_0/4$ to $4\mu_0$, i.e. ranging from approximately 20 GeV to 360 GeV. The combined PDF and α_s uncertainty is assessed by comparing the nominal CTEQ6.6 prediction with the results obtained for NNPDF2.1 and MSTW08, while m_b is varied from 4.2 GeV to 5 GeV.

Acknowledgments

We would like to thank Tobias Golling and Andrea Messina from the ATLAS collaboration for many fruitful discussions and for providing us all the information necessary to obtain the results presented in this paper. L.R. and D.W. thank the Kavli Institute for Theoretical Physics (KITP) for the kind hospitality extended to us while this work was being

Table 10: b-jet cross sections (in pb) for $W+1$ and $W+2$ jet production where at least one jet is a b jet, LHC ($\sqrt{s} = 7$ TeV). No branching ratios or tagging efficiencies are included. The Monte Carlo integration error is 0.5%.

	$\sigma_{b-\text{jet}}(W^+)$	$\sigma_{b-\text{jet}}(W^-)$
$\mu = \mu_0/4$	90.5	55.4
$\mu = \mu_0/2$	79.5	48.9
$\mu = \mu_0$	72.6	44.5
$\mu = 2\mu_0$	66.6	40.8
$\mu = 4\mu_0$	61.6	37.7

completed. The work of L.R. is supported in part by the U.S. Department of Energy under grant DE-FG02-97IR41022. The work of D.W. is supported in part by the National Science Foundation under grants NSF-PHY-0547564 and NSF-PHY-0757691. Fermilab is operated by Fermi Research Alliance, LLC under Contract No. DE-AC02-07CH11359 with the United States Department of Energy. This research was supported in part by the National Science Foundation under Grant No. NSF PHY05-51164 and by a US-Italy Fulbright Visiting Student Researcher Fellowship.

References

[1] R. K. Ellis and S. Veseli, Phys. Rev. D **60**, 011501 (1999) [arXiv:hep-ph/9810489].

[2] F. Febres Cordero, L. Reina and D. Wackeroth, Phys. Rev. D **74**, 034007 (2006) [arXiv:hep-ph/0606102].

[3] S. Badger, J. M. Campbell and R. K. Ellis, JHEP **1103**, 027 (2011) [arXiv:1011.6647 [hep-ph]].

[4] R. Frederix, S. Frixione, V. Hirschi, F. Maltoni, R. Pittau and P. Torrielli, arXiv:1106.6019 [hep-ph].

[5] J. Campbell, R. K. Ellis, F. Maltoni and S. Willenbrock, Phys. Rev. D **75**, 054015 (2007) [arXiv:hep-ph/0611348].

[6] C. Oleari and L. Reina, [arXiv:1105.4488 [hep-ph]].

[7] J. Campbell and R. K. Ellis, MCFM - Monte Carlo for FeMtobarn processes, http://mcfm.fnal.gov/.

[8] J. M. Campbell, R. K. Ellis, F. Febres Cordero, F. Maltoni, L. Reina, D. Wackeroth and S. Willenbrock, Phys. Rev. D **79**, 034023 (2009) [arXiv:0809.3003 [hep-ph]].

[9] M. A. G. Aivazis, J. C. Collins, F. I. Olness and W. K. Tung, Phys. Rev. D **50**, 3102 (1994) [arXiv:hep-ph/9312319].

[10] J. C. Collins, Phys. Rev. D **58**, 094002 (1998) [arXiv:hep-ph/9806259].

[11] G. Aad *et al.* [ATLAS Collaboration], Phys. Lett. B **707**, 418 (2012) [arXiv:1109.1470 [hep-ex]].

[12] F. F. Cordero, L. Reina and D. Wackeroth, PoS **RADCOR2009**, 055 (2010) [arXiv:1001.3362 [hep-ph]].

[13] J. Campbell, F. Febres Cordero, L. Reina, private communication.

[14] T. Aaltonen *et al.* [CDF Collaboration], arXiv:0909.1505 [hep-ex].

[15] P. M. Nadolsky, H. -L. Lai, Q. -H. Cao, J. Huston, J. Pumplin, D. Stump, W. -K. Tung, C. -P. Yuan, Phys. Rev. **D78**, 013004 (2008). [arXiv:0802.0007 [hep-ph]].

[16] H. -L. Lai, J. Huston, Z. Li, P. Nadolsky, J. Pumplin, D. Stump and C. -P. Yuan, Phys. Rev. D **82**, 054021 (2010) [arXiv:1004.4624 [hep-ph]].

[17] R. D. Ball, L. Del Debbio, S. Forte, A. Guffanti, J. I. Latorre, J. Rojo and M. Ubiali, Nucl. Phys. B **838**, 136 (2010) [arXiv:1002.4407 [hep-ph]].

[18] A. D. Martin, W. J. Stirling, R. S. Thorne and G. Watt, Eur. Phys. J. C **63**, 189 (2009) [arXiv:0901.0002 [hep-ph]].

[19] M. Botje *et al.*, arXiv:1101.0538 [hep-ph].